Cell Reports
Article

Rewiring AMPK and Mitochondrial Retrograde Signaling for Metabolic Control of Aging and Histone Acetylation in Respiratory-Defective Cells

R. Magnus N. Friis,[1] John Paul Glaves,[1] Tao Huan,[2] Liang Li,[2] Brian D. Sykes,[1] and Michael C. Schultz[1,*]
[1]Department of Biochemistry, University of Alberta, Edmonton, AB T6G 2H7, Canada
[2]Department of Chemistry, University of Alberta, Edmonton, AB T6G 2H7, Canada
*Correspondence: michael.schultz@ualberta.ca
http://dx.doi.org/10.1016/j.celrep.2014.03.029

SUMMARY

Abnormal respiratory metabolism plays a role in numerous human disorders. We find that regulation of overall histone acetylation is perturbed in respiratory-incompetent (ρ^0) yeast. Because histone acetylation is highly sensitive to acetyl-coenzyme A (acetyl-CoA) availability, we sought interventions that suppress this ρ^0 phenotype through reprogramming metabolism. Nutritional intervention studies led to the discovery that genetic coactivation of the mitochondrion-to-nucleus retrograde (RTG) response and the AMPK (Snf1) pathway prevents abnormal histone deacetylation in ρ^0 cells. Metabolic profiling of signaling mutants uncovered links between chromatin-dependent phenotypes of ρ^0 cells and metabolism of ATP, acetyl-CoA, glutathione, branched-chain amino acids, and the storage carbohydrate trehalose. Importantly, RTG/AMPK activation reprograms energy metabolism to increase the supply of acetyl-CoA to lysine acetyltransferases and extend the chronological lifespan of ρ^0 cells. Our results strengthen the framework for rational design of nutrient supplementation schemes and drug-discovery initiatives aimed at mimicking the therapeutic benefits of dietary interventions.

INTRODUCTION

Abnormal mitochondrial function is implicated in aging and a broad spectrum of disease mechanisms (Greaves et al., 2012). Beyond the energy defects associated with respiratory deficiency, the loss of cells with abnormal mitochondria causes many of the clinical symptoms, including organ failure, that are associated with mitochondrial disease (Wallace et al., 2010). The development of strategies to maintain the viability of cells with respiratory defects is therefore of great interest.

Chromatin regulation is likely tied to respiratory activity by two metabolic dependencies. First, lysine acetyltransferases (KATs) require acetyl-coenzyme A (acetyl-CoA) as a cofactor, and H3-H4 acetylation in yeast and humans is directly controlled by acetyl-CoA availability (Friis et al., 2009; Morrish et al., 2010; Takahashi et al., 2006; Wellen et al., 2009). Second, acetyl-CoA synthesis requires ATP. It follows that overall histone acetylation is linked to control of the energy state of the cell. We obtained support for this model by revealing a molecular circuitry in which glucose regulation of histone acetylation depends on respiratory function and can be controlled by modulation of signaling pathways that regulate mitochondrial biogenesis and metabolic reprogramming in cells lacking mtDNA. We show that components of this circuitry affect chronological aging and the intracellular levels of metabolites that are implicated in aging.

RESULTS AND DISCUSSION

mtDNA Status Influences Glucose Regulation of Overall H4 Acetylation

In the course of progression into stationary phase (SP), yeast cells with functional mitochondria deplete exogenous nutrients and switch from glycolysis to energy production by oxidative phosphorylation (Zaman et al., 2008). This switch is not executed by ρ^0 cells, which lack the respiratory proteins encoded by the mitochondrial genome. In SP, the overall level of tetra-acetylated H4 is markedly lower in ρ^0 cells than in ρ^+ cells (Figure 1A, "pan-H4ac") because of lower acetylation at K5, K8, and K12, but not K16 (Figure 1A). Deacetylation of H3 K9 during SP entry is also more pronounced in ρ^0 cells than in ρ^+ cells (Figure S1A). Because there is no global downregulation of H3 or H4 in ρ^0 cells (Figures 1A and S1A), histone proteolysis is not responsible for their "loss of acetylation" phenotype.

While cells are proliferating in glucose-rich medium, oxidative phosphorylation is repressed and mtDNA status has little effect on H4 tail acetylation (Figure 1B, lanes 1 and 2). Glucose starvation of highly proliferative ρ^0 cells, however, triggers H4 deacetylation (Figure 1B, compare lanes 2 and 4), and glucose in the absence of other major nutrients can maintain acetylation in ρ^+ and ρ^0 cells (Figure 1B, lanes 9 and 10). Nitrogen starvation does not affect H4 acetylation in ρ^0 cells (Figure 1B, compare lanes 2 and 12). Therefore, maintenance of histone acetylation depends almost exclusively on glucose. The glucose analog 2-deoxy-D-glucose (2-DG) is imported by cells but cannot be

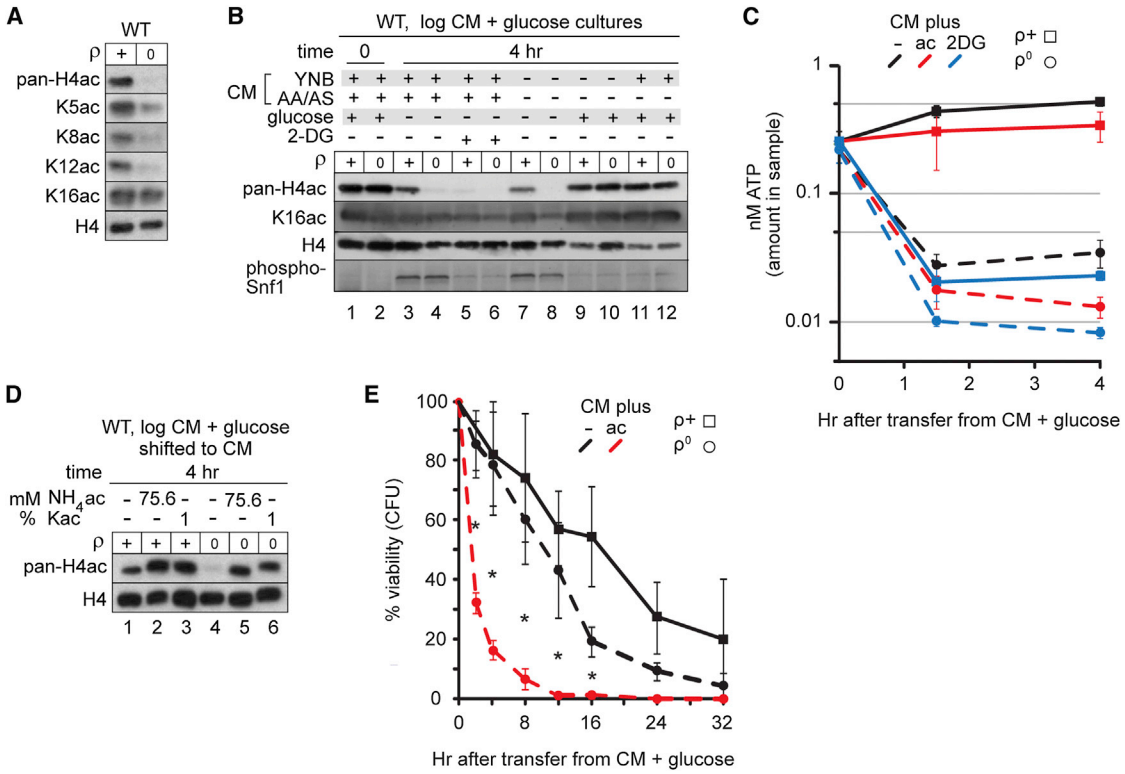

Figure 1. Nutrient Regulation of H4 Tail Acetylation in Cells with and without mtDNA

H4 acetylation was probed using a pan-specific tail antibody (pan-H4ac) or antibodies indicated by lysine numbering on the left. All error bars represent SD (n = 3).

(A) H4 acetylation in cells cultured for 7 days in rich starting medium (YPD; yeast extract bactopeptone 2% glucose).

(B) Effects of glucose and nitrogen source (YNB, yeast nitrogen base; AA/AS, amino acids/ammonium sulfate) availability, and 2-DG on H4 acetylation in proliferating cells. CM, complete minimal medium.

(C) Relative cellular content of ATP determined by an enzyme-coupled assay.

(D) Acetate suppresses loss of H4 acetylation in ρ^0 cells. Actively growing cells were shifted to CM with or without acetate.

(E) Acetate causes inviability. For each starting condition, viability at transfer to medium without acetate is set to 100%. For the comparison between ρ^0 cells in CM and CM + acetate (asterisks), $p < 0.025$. CFU, colony-forming units.

fully metabolized (Coons et al., 1995; Wilson et al., 1996). Because 2-DG does not protect H4 from deacetylation in ρ^+ or ρ^0 cells switched out of glucose-rich medium (Figure 1B, lanes 5 and 6), histone acetylation is supported by metabolism of glucose, rather than uptake-dependent intracellular signaling. Moreover, given that ATP depletion results from 2-DG metabolism (Figure 1C) (Wilson et al., 1996), H4 deacetylation in 2-DG may be due to inhibition of ATP-dependent events that govern the balance between KAT and histone deacetylase (HDAC) activities.

Disruption of ATP Metabolism Is Not the Sole Cause of Abnormal Glucose Regulation of Histone Acetylation in ρ^0 Cells

The predominant phenotype of ρ^0 cells is loss of respiratory capacity. We hypothesized that this defect in carbon metabolism underlies abnormal regulation of histone acetylation in ρ^0 cells, encouraged by the fact that neither ongoing mRNA transcription nor translation is required for (1) short-term (4 hr) maintenance of acetylation in ρ^+ cells or (2) loss of acetylation in ρ^0 cells under glucose limitation (Figures S1E and S1F).

The global level of histone acetylation is defined by the balance between ongoing histone acetylation by KATs and deacetylation by HDACs. Maintenance of the overall histone acetylation level therefore requires a continual supply of acetyl-CoA. In yeast, the acetyl-CoA that is utilized by KATs to drive histone acetylation is supplied by the ATP-dependent activation of acetate to acetyl-CoA (Takahashi et al., 2006). To investigate the possibility that abnormal carbon metabolism underlies differential regulation of H4 acetylation, we examined the effect of supplying exogenous acetate to cells after glucose removal. Comparison of H4 acetylation in ρ^+ and ρ^0 cells switched from complete minimal medium (CM) + glucose to CM or CM + acetate revealed that acetate blocks the H4 deacetylation seen in ρ^0 cells subjected to glucose limitation (Figure 1D). Interestingly, although exogenous acetate allows ρ^0 cells to maintain histone acetylation in the absence of glucose, it causes rapid cell death (Figure 1E). These findings are in line with evidence that acetic acid accelerates chronological aging of wild-type cells (Burtner et al., 2009). We speculated that this effect might be associated with ATP depletion, because acetate cannot be used by ρ^0 cells to generate ATP (Flores et al., 2000; Minard and McAlister-Henn,

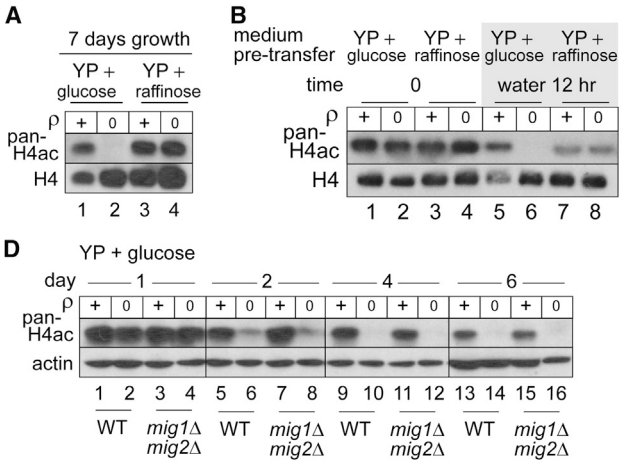

Figure 2. Metabolic Reprogramming of H4 Acetylation in ρ^0 Cells

(A) Progression of raffinose-grown cells into SP is not associated with loss of H4 acetylation.

(B) Preculture in raffinose suppresses loss of H4 acetylation in ρ^0 cells shifted to water. This suppression was observed in all replicate experiments, despite some variability between glucose- and raffinose-grown ρ^+ cells in their response to carbon-source withdrawal.

(C and D) Mutations in the carbon catabolite repression pathway do not affect loss of H4 acetylation.

Immunoblotting as in Figure 1.

2010) but can be used for other processes that consume ATP. Consistent with this idea, in ρ^0 cells, acetate supplementation led to an even greater depletion of ATP than was evident in CM without a carbon source (Figure 1C, $p = 0.0447$ at 4 hr).

We further examined the alternate possibility that rather than modulating carbon metabolism, acetate affects H4 acetylation by inhibiting HDAC activity. Although acetate can inhibit HDAC activity in vitro (Carmen et al., 1996) and HDAC (Rpd3) deletion affects regulation of H4 acetylation in ρ^0 cells subjected to glucose deprivation (Figure S2A), acetate does not prevent H4 deacetylation caused by inactivation of the major H4 KAT Esa1 (Figure S2B). Therefore, acetate most likely protects H4 from deacetylation in ρ^0 cells by a mechanism that increases KAT activity, but not the supply of ATP. Together, these results suggest that ATP insufficiency does not fully account for anomalous H4 deacetylation in ρ^0 cells.

If loss of mtDNA causes loss of H4 acetylation by disrupting central carbon metabolism, then corruption of signaling that controls respiratory capacity might cause the same phenotype. To explore this possibility, H4 acetylation was studied in ρ^+ cells lacking Snf1, a major regulator of respiratory program induction in response to glucose removal and the equivalent of mammalian AMP-dependent protein kinase (AMPK) (Mayer et al., 2011; Hedbacker and Carlson, 2008). Consistent with a causal relationship between abnormal Snf1 signaling and abnormal regulation of histone acetylation in ρ^0 cells, deletion of *SNF1* and other genes required for growth on nonfermentable carbon sources has the same deleterious effect on maintenance of acetylation as loss of mtDNA (Figures S1B–S1D). Furthermore, 2-DG blocks maintenance of histone acetylation in ρ^+ cells and does not support activating Thr210 phosphorylation of Snf1 (Figure 1B, top and bottom panels). Both the Hardie and Carlson labs have reported that although 2-DG depletes ATP, it blocks activation of Snf1. These groups attributed failure of Snf1 activation to severe ATP depletion (Hedbacker and Carlson, 2006; Wilson et al., 1996). We also readily detected ATP depletion upon 2-DG treatment (Figure 1C). Notably, the extent of ATP depletion caused by 2-DG supplementation during glucose starvation in either ρ^+ or ρ^0 cells is greater than in ρ^0 cells after glucose removal (Figure 1C, at 4 hr: ρ^0 CM versus ρ^+ 2-DG, $p = 0.0011$; ρ^0 CM versus ρ^0 2-DG, $p = 0.0316$). Collectively, this evidence encourages the view that disruption of Snf1 signaling contributes to abnormal histone deacetylation in ρ^0 cells. Surprisingly, however, Snf1 is Thr210 phosphorylated in response to glucose withdrawal regardless of mtDNA status (Figure 1B). In other words, phosphorylation-dependent Snf1 activation is not the target of mechanisms that cause loss of acetylation in ρ^0 cells during glucose deprivation.

A Sugar Substitution Protects H4 Acetylation in ρ^0 Cells

Glucose activates "carbon catabolite repression" (CCR), which suppresses genes required for respiratory metabolism, gluconeogenesis, and the utilization of poor carbon sources (Schüller, 2003). The fermentable trisaccharide raffinose supports growth of ρ^0 cells without establishment of CCR (Epstein et al., 2001) and allows them to maintain histone acetylation at near ρ^+ levels (Figure 2A) even after 12 hr in water (Figure 2B, compare lanes 7 and 8). We conclude that cells without mtDNA can set up a program of physiology that supports the maintenance of H4 acetylation even though they cannot generate ATP by oxidative phosphorylation.

Physiological reprogramming governed by carbon-source availability depends critically on Snf1, its inactivating phosphatase (Glc7 in complex with a regulatory subunit, Reg1) (Hedbacker and Carlson, 2008), and its transcription factor targets Mig1 and Mig2 (phosphorylation of Mig1/Mig2 by Snf1 relieves their repression of genes involved in utilization of alternative carbon sources, oxidative phosphorylation, and gluconeogenesis) (Smets et al., 2010; Zaman et al., 2008). Unlike raffinose (Figure 2A, compare lanes 2 and 4), which activates Snf1 in association with relief of CCR, neither constitutive activation of Snf1 by *REG1* deletion (Figure 2C, compare lanes 2 and 5) nor simultaneous deletion of *MIG1* and *MIG2* (Figure 2D) prevents loss of acetylation in ρ^0 cells grown on glucose. Although loss of Snf1 phenocopies H4 deacetylation associated with mtDNA loss (Figures S1B and S1C), Snf1 function in this regulatory capacity (1) is not executed exclusively in the context of the signaling program defined by Reg1 and Mig1/Mig2 and (2) does not explain how raffinose suppresses loss of H4 acetylation in ρ^0 cells (Figures 2A and 2B). The protective effect of raffinose on H4 acetylation likely requires Snf1-independent signaling that is sensitive to nutrients or mitochondrial activity

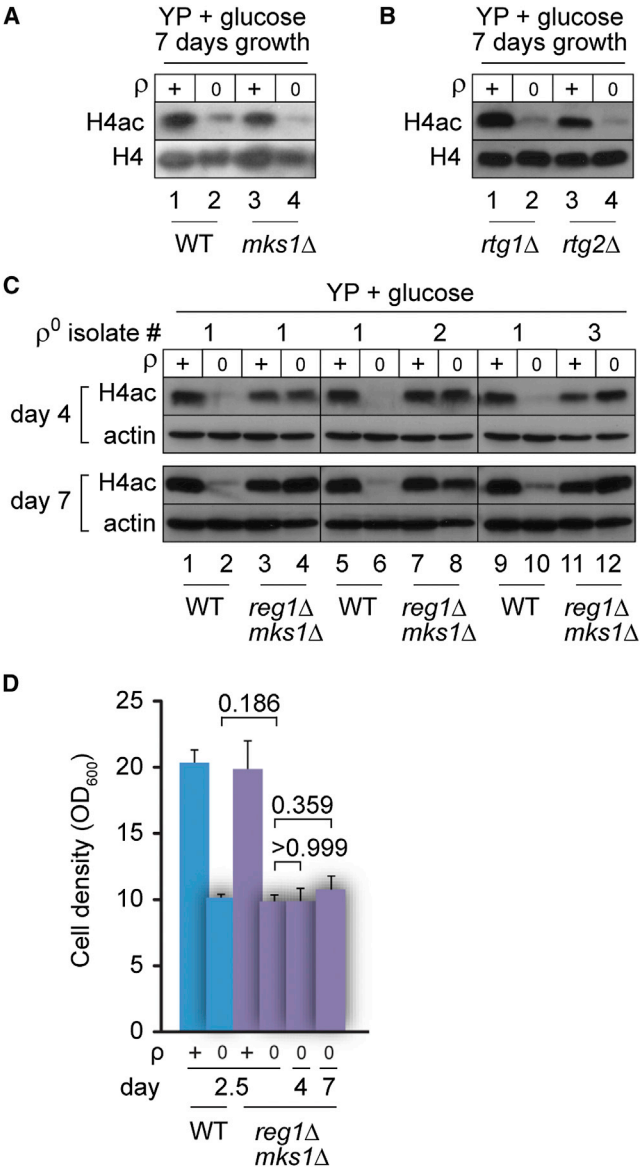

Figure 3. Reconfiguration of Snf1 and RTG Signaling Suppresses Loss of H4 Acetylation in ρ^0 Cells

(A and B) Loss of H4 acetylation during progression into SP is not affected by activation (A) or inhibition (B) of RTG signaling.

(C) Simultaneous activation of Snf1 and RTG signaling suppresses loss of H4 acetylation in ρ^0 cells cultured into SP in YPD.

(D) The proliferation capacity of ρ^0 cells is not affected by simultaneous activation of Snf1 and RTG signaling. The error bars represent SD (day 2.5, n = 11; days 4 and 7, n = 3).

Immunoblotting as in Figure 1.

and may function alone or in concert with Snf1 to protect histone acetylation in ρ^0 cells.

Constitutive Activation of AMPK and RTG Signaling Protects H4 Acetylation in ρ^0 Cells

Based on the known metabolic and signaling inputs to genes that are misregulated in ρ^0 cells (Epstein et al., 2001; Zaman et al., 2008), we identified four pathways to test for involvement in control of H4 deacetylation in ρ^0 cells: the target of rapamycin (TOR) pathway, the unfolded protein response (UPR) pathway, the pleiotropic drug-resistance (PDR) pathway, and the retrograde response pathway (Butow and Avadhani, 2004; Hallstrom and Moye-Rowley, 2000; Ron and Walter, 2007; Smets et al., 2010; Zaman et al., 2008). We could not demonstrate an effect of any single pathway on programming of H4 deacetylation in ρ^0 cells. Data for the TOR, UPR, and PDR pathways are shown in Figure S3. Figure 3 shows the effect of RTG dysregulation (Liu et al., 2003). Despite the fact that RTG activation allows ρ^0 cells to reconfigure metabolism in a way that partly compensates for defects in mitochondrial function (Butow and Avadhani, 2004), neither constitutive activation in *mks1Δ* cells (Figure 3A) nor inactivation in *rtg1Δ* and *rtg2Δ* cells (Figure 3B) affects ρ^+ or ρ^0 programming of H4 deacetylation during SP.

Previous work revealed that induction of some RTG genes during growth on raffinose depends on synergy between RTG signaling effectors and transcription proteins activated by Snf1-dependent signaling (Liu and Butow, 1999). We find that simultaneous deletion of *REG1* to activate Snf1, and deletion of *MKS1* to activate the RTG response, allows ρ^0 cells cultured into SP to maintain histone acetylation at the level observed in ρ^+ wild-type and *reg1Δ mks1Δ* cells (Figure 3C). This restoration of H4 acetylation was not simply a passive result of an effect on proliferation, because simultaneous deletion of *REG1* and *MKS1* did not improve population expansion of ρ^0 cells (Figure 3D). Overall, our results suggest (1) that abnormal carbon metabolism underlies loss of H4 acetylation in ρ^0 cells and (2) that this metabolic supply defect can be suppressed by combined rewiring of Snf1 signaling and activation of the RTG pathway that signals information about the functional status of the mitochondrion to the nucleus.

Constitutive Activation of AMPK and RTG Signaling in ρ^0 Cells Increases the Supply of Acetyl-CoA for Histone Acetylation

Information about the dynamics of histone acetylation in SP and the regulation of acetyl-CoA abundance during progression into SP suggested a way to test if *MKS1 REG1* double deletion protects overall acetylation in SP ρ^0 cells by a metabolic mechanism. The data we have presented demonstrate that unlike their ρ^0 counterparts, ρ^+ cells are capable of maintaining H4 acetylation during SP or following removal of glucose from their growth media. Impressively, the level of overall histone acetylation remains relatively high despite massive declines in cellular acetyl-CoA abundance. Studies employing reversed-phase ion-pair high-performance liquid chromatography (HPLC) have demonstrated that the free pool of acetyl-CoA declines markedly between log phase growth and SP (Seker et al., 2005). Somewhat surprisingly, at least from an energetic standpoint, during SP when extracellular nutrients are scarce, the maintenance of acetylation is not simply achieved by downregulation of HDAC activity. During SP, protein levels of the HDAC Rpd3 are kept high and deletion of *RPD3* results in elevated histone acetylation in ρ^+ cells (Friis et al., 2009; Sandmeier et al., 2002). Maintenance of histone acetylation appears to require ongoing ATP-dependent synthesis of acetyl-CoA, which is utilized by KATs for

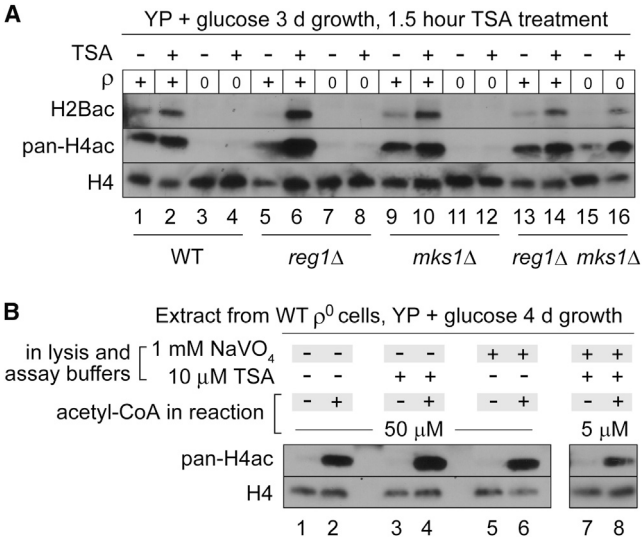

Figure 4. Relationship between Histone Acetylation and Acetyl-CoA Supply in ρ^0 Cells

(A) Effect of HDAC inhibition on histone acetylation in vivo.

(B) In vitro KAT activity.

de novo histone acetylation. In ρ^+ cells during SP, inhibition of the major H4 KAT Esa1, or simultaneous inactivation of acetyl-CoA synthases Acs1 and Acs2, which supply the acetyl-CoA used by KATs, results in loss of histone acetylation (Friis et al., 2009). Despite the inherent energetic cost, dynamic regulation of overall histone acetylation is likely advantageous in SP, because untargeted and targeted acetylation are important for regulation of transcription (reviewed in Friis and Schultz 2009) and intracellular pH (McBrian et al., 2013). Based on this information about dynamic interplay between KATs and HDACs, we further examined control of overall histone acetylation in SP ρ^0 cells lacking *REG1* and *MKS1*. We first took advantage of the ability to manipulate HDAC activity by a pharmacological method, reasoning that if a population of cells has catalytically active KATs and a sufficient supply of acetyl-CoA, then inhibition of HDACs should result in increased overall histone acetylation. HDAC inhibition was achieved by treating SP cells with trichostatin A (TSA). Figure 4A shows the data for H4 and H2B acetylation (note that the pan-H4ac antibody also detects acetylated H2B [see Table S2] and that H2B acetylation is not readily detectable during SP without TSA treatment). TSA stimulates overall histone acetylation in SP ρ^+ cells (Figure 4A, compare lanes 1 and 2, 5 and 6, 9 and 10, and 13 and 14), but not ρ^0 wild-type, *reg1Δ* or *mks1Δ* cells (Figure 4A, lanes 3 and 4, 7 and 8, and 11 and 12); the implication of this result is that KAT activity or the supply of acetyl-CoA for histone acetylation is compromised in these ρ^0 strains. On the other hand, TSA treatment is associated with robust induction of H4 and H2B acetylation in ρ^0 cells lacking both *REG1* and *MKS1* (Figure 4A, compare lanes 15 and 16). This strongly suggests that ρ^0 *reg1Δ mks1Δ* cells possess catalytically active KATs and a sufficient supply of acetyl-CoA for KAT function.

Theoretically, the results in Figure 4A do not rule out the possibility that there is an essential signaling component to regulation of KAT activity in SP ρ^0 cells. For example, a signaling event (activated specifically in ρ^0 cells during SP or after glucose removal) could inhibit the catalytic activity of KATs. This type of mechanism could prevent ρ^0 cells from increasing histone acetylation after inhibition of HDACs, independently of changes in the supply of acetyl-CoA. Furthermore, this inhibitory signaling might not occur in ρ^0 cells lacking both *REG1* and *MKS1*.

To explore the hypothesis that loss of mtDNA status somehow inhibits intrinsic KAT activity, we employed a crude yeast extract to directly assay histone acetylation by KATs from SP ρ^0 cells (method modified from Mullen et al., 1989). This extract is depleted of many soluble proteins and soluble metabolites such as acetyl-CoA but contains the histones and multiple KAT activities. A phosphatase inhibitor and TSA were included in the preparation of some extracts and in the reactions in which these extracts were used. Although TSA could improve detection of acetylation by counteracting the direct effects of HDACs on histone acetylation, this was not only one reason for its inclusion. Signaling events could potentially affect the phosphorylation or acetylation state of KAT complexes. Both marks have been demonstrated to affect KAT activity and have been observed in yeast KAT complexes. Esa1 acetyltransferase activity is regulated by autoacetylation (Yuan et al., 2012), the human counterpart of Esa1 (Tip60) is regulated by phosphorylation (Lemercier et al., 2003), and Esa1 and several components of the complexes in which it resides are phosphorylated in vivo (Allard et al., 1999; Boudreault et al., 2003; phosphoprotein database of Sadowski et al., 2013). TSA and sodium orthovanadate were therefore included to reduce the likelihood of changes in the native acetylation and phosphorylation state of the KAT complexes in extracts from SP ρ^0 cells. Our KAT assay involved addition of acetyl-CoA or vehicle to cell extract, followed by incubation at 37°C for 20 min. We used relatively high acetyl-CoA concentrations, because the extract lacks the components necessary to replenish acetyl-CoA by synthesis and the substrate histones in ρ^0 extracts are largely deacetylated. Much lower concentrations of acetyl-CoA probably suffice for maintenance of acetylation in vivo, where ongoing synthesis need only supply enough acetyl-CoA to allow the rate of histone acetylation to keep pace with the rate of deacetylation. Proteins isolated from the reactions were analyzed by immunoblotting using the tetra-acetylated and bulk H4 antibodies. In reactions that did not receive acetyl-CoA, probing with the pan-H4ac antibody yielded only a weak signal (Figure 4B, lanes 1, 3, 5, and 7). By comparison, pan-H4ac reactivity was very strong in all assays supplemented with 50 μM acetyl-CoA whether extracts were prepared and assayed with or without TSA or phosphatase inhibitors (Figure 4B, compare lanes 1 and 2, 3 and 4, and 5 and 6). Acetylation was also evident when acetyl-CoA was provided at one-tenth the concentration (5 μM) in the presence of both TSA and phosphatase inhibitor (Figure 4B, lanes 7 and 8). These results demonstrate the existence of active KATs in SP ρ^0 cells and, together with the data on the in vivo effects of TSA (Figure 4A), strongly support the model that rewiring of Snf1 signaling and activation of the RTG pathway rescues the histone deacetylation phenotype of ρ^0 cells at least partly by increasing the supply of acetyl-CoA for use by KATs.

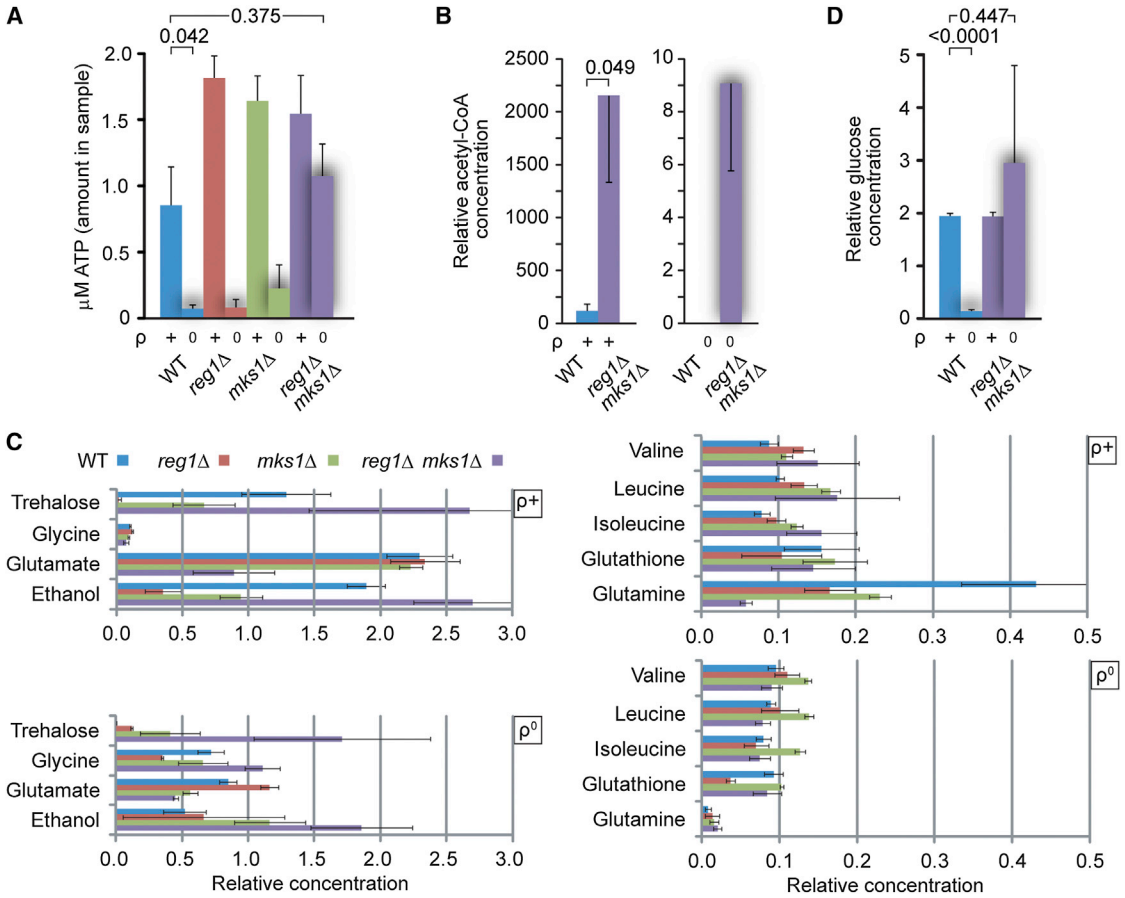

Figure 5. Metabolic Effects of Activation of Snf1 Signaling and the RTG Response Pathway

(A) Relative concentration of ATP in equivalent samples.

(B) Relative cellular content of acetyl-CoA determined by LC-MS/MS. Acetyl-CoA was undetectable in wild-type ρ^0 cells.

(C) ^{1}H-NMR metabolite profiling.

(D) Relative cellular content of glucose determined by ^{1}H-NMR spectroscopy.

All error bars represent SD (n = 3).

AMPK and RTG Signaling Modulate the Metabolomes of ρ^+ and ρ^0 Cells and Their Aging

Under a metabolic model for suppression of the histone acetylation phenotype of ρ^0 cells, *reg1Δ* combined with *mks1Δ* is predicted to shift carbon metabolism of wild-type ρ^0 cells toward that of ρ^+ cells. More specifically, deletion of *REG1* together with *MKS1* is expected to increase the supply of acetyl-CoA to KATs by a metabolic mechanism that includes stimulation of ATP generation for use in acetyl-CoA synthesis. Direct measurements indeed revealed that combined, but not individual, deletion of *REG1* and *MKS1* allows ρ^0 cells to maintain ATP levels similar to those seen in wild-type ρ^+ cells (Figure 5A). Liquid chromatography-tandem mass spectrometry (LC-MS/MS) was used to measure acetyl-CoA abundance in SP wild-type and *reg1Δ mks1Δ* cells, either with or without mtDNA (Figure 5B). Deletion of *REG1* and *MKS1* in ρ^+ cells is associated with a 12-fold increase in acetyl-CoA abundance. Therefore, *REG1* and *MKS1* are components of a system that can control the cellular supply of acetyl-CoA. Histone acetylation in ρ^+ cells is not boosted by loss of *REG1* and *MKS1* (Figure 3C) and therefore is not limited by the supply of acetyl-CoA. The opposite is highly probable in ρ^0 cells, because histone acetylation and acetyl-CoA abundance are both increased in the absence of *REG1* and *MKS1* (Figures 3C and 5B, respectively), and the H4-directed KATs of ρ^0 cells are stimulated by an increased supply of acetyl-CoA in vitro (Figure 4B). Therefore, even in ρ^0 cells that cannot mobilize mitochondrial mechanisms of central carbon metabolism, combined activation of Snf1 and RTG signaling can increase the supply of acetyl-CoA for use by KATs.

Clues about how altered Snf1 and RTG signaling affects metabolic pathways connected to acetyl-CoA availability were obtained by proton nuclear magnetic resonance (^{1}H-NMR) metabolic profiling. Specifically, we compared the abundance of a panel of intracellular metabolites in ρ^+ and ρ^0 wild-type, *reg1Δ*, *mks1Δ*, and *reg1Δ mks1Δ* cells after 2.5 days growth in rich medium (YPD). Figure 5C shows concentrations of selected metabolites relative to a reference library. The metabolite changes revealed by ^{1}H-NMR suggest a plausible working model for the chain of metabolic events that underlie increases in the supply of ATP (Figure 5A) and acetyl-CoA (Figure 5B) in

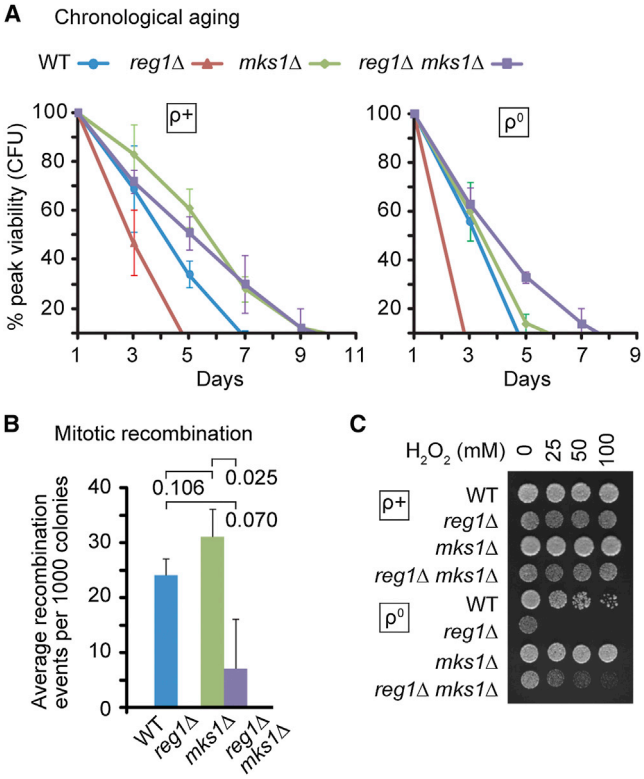

Figure 6. Physiological Effects of Activation of Snf1 Signaling and the RTG Response Pathway

(A) Chronological aging of cells in batch culture. Statistical analysis of differences between strains at 5 days: wild-type ρ^+ versus ρ^0, p = 0.009; wild-type ρ^+ versus *reg1Δ mks1Δ* ρ^0, p = 0.730; wild-type ρ^+ versus *mks1Δ* ρ^+, p = 0.009; *reg1Δ* ρ^+ versus *reg1Δ mks1Δ* ρ^0, p = 0.005.

(B) Recombination in the rDNA array.

(C) Oxidative stress resistance of SP cells.

All error bars represent SD (n = 3).

ρ^0 cells lacking *MKS1* and *REG1* (Figure S4A summarizes additional metabolite changes and their possible physiological significance). The metabolite trehalose figures prominently in this model. Trehalose is a glucose polymer that functions as a storage carbohydrate and extends chronological lifespan (Kyryakov et al., 2012; Ocampo et al., 2012). It is broken down to glucose by two trehalases (Nwaka and Holzer, 1998). Glucose in turn yields ATP and pyruvate by way of glycolysis, and acetaldehyde generated from pyruvate can yield acetate in a reaction catalyzed by aldehyde dehydrogenase (Fraenkel, 1982). We speculate that this program of events supports higher production of acetyl-CoA in *reg1Δ mks1Δ* cells lacking mtDNA, for the following reasons. First, trehalose depletion is observed in wild-type cells without mtDNA (see also Enjalbert et al., 2000), but not in cells lacking *MKS1* and *REG1* (Figure 5C; trehalose is undetectable in wild-type ρ^0 cells and has similar abundance in wild-type ρ^+ and *reg1Δ mks1Δ* cells, p = 0.3834). ρ^0 *reg1Δ mks1Δ* cells therefore enter SP with a trehalose store that we propose is used to boost the availability acetyl-CoA for histone acetylation. Second, deletion of *REG1* and *MKS1* in ρ^0 cells restores glucose to the level observed in wild-type ρ^+ cells (Figure 5D). We propose that trehalose breakdown accounts for this effect in ρ^0 *reg1Δ mks1Δ* cells.

Reprogramming of intracellular signaling can correct a chromatin perturbation in ρ^0 cells that likely stems from abnormal energy metabolism centered on glucose and its storage form that promotes longevity in SP. Therefore, mutations that affect glucose control of histone acetylation were assessed for their effect on chronological aging (Fabrizio and Longo, 2003; Wei et al., 2011) and biochemical pathways associated with this process. Most importantly, the only genetic alteration that protects H4 acetylation in ρ^0 cells, simultaneous deletion of *REG1* and *MKS1*, also restores the lifespan of ρ^0 cells to that of wild-type ρ^+ cells (Figure 6A, compare day of 10% viability for wild-type [blue] and *reg1Δ mks1Δ* [purple]; see also Figure S4B). Deletion of *MKS1* alone extends the chronological lifespan of ρ^+ cells (Figure 6A, left), and dramatically suppresses the premature aging of *reg1Δ* single mutants (Figure 6A). The extended lifespan of respiratory-competent *mks1Δ* mutants is separable from trehalose metabolism; *mks1Δ* cells have lower trehalose levels than wild-type (Figure 5C). The mechanism of this lifespan extension is unknown, although it is plausible that metabolism of branched chain amino acids (BCAAs; valine, leucine, and isoleucine) plays a role. BCAA levels are elevated in *mks1Δ* cells (Figure 5C; ρ^+ wild-type versus *mks1Δ*: valine p = 0.052; leucine p = 0.005; isoleucine p = 0.004). Because all strains are *leu2Δ0* and incapable leucine synthesis, its accumulation is due to increased uptake/storage, and/or lower catabolism. This BCAA accumulation may contribute to lifespan extension, given that (1) leucine prolongs yeast chronological viability (Alvers et al., 2009), (2) BCAA elevation is a hallmark of genetically diverse long-lived *Caenorhabditis elegans* mutants (Fuchs et al., 2010; Martin et al., 2011), and (3) BCAA supplementation extends the median lifespan of middle-aged mice (D'Antona et al., 2010).

Alone and in combination, the genetic manipulations that we show affect metabolic control of histone acetylation also affect physiological mechanisms that are important in aging. Recombination in the rDNA array (Roy and Runge, 2000; Sinclair and Guarente, 1997) is controlled by chromatin silencing involving H3 and H4 deacetylation and the NAD^+-dependent HDAC Sir2, which also controls replicative aging (Bryk et al., 1997; Gottlieb and Esposito, 1989; Sinclair and Guarente, 1997; Smith and Boeke, 1997). We find that *REG1* deletion strongly inhibits rDNA recombination in actively proliferating ρ^+ cells by a mechanism that partly requires *MKS1* (Figure 6B; technical issues precluded analysis of ρ^0 cells; see Supplemental Information). Oxidative stress resistance is intimately linked to control of chronological lifespan and partly depends on orderly transcriptional regulation of stress response genes (Petti et al., 2011). Regardless of *MKS1/REG1* genotype, ρ^0 cells are more sensitive to oxidative stress caused by H_2O_2 than their ρ^+ counterparts (Figures 6C and S4C). Resistance to oxidants strongly depends on conversion of glutathione to glutathione disulfide, and elevation of the glutathione disulfide to glutathione ratio in the cell is indicative of oxidative stress (Morano et al., 2012). While glutathione disulfide was not among the metabolites in the library used for metabolite identification by ^{1}H-NMR, changes in the abundance of glutathione (Figure 5C) hint at a metabolic mechanism for the high sensitivity of *reg1Δ* ρ^0 cells to H_2O_2 (Figure 6C). Specifically,

reg1Δ had the lowest level of glutathione of any ρ^0 strain (Figure 5C; p values < 0.0001–0.013 for glutathione in *reg1Δ* ρ^0 versus other ρ^0 strains).

Conclusions

Our studies show that artificial coactivation of Snf1 signaling and the RTG response in *reg1Δ mks1Δ* cells mimics the protection of histone acetylation afforded to ρ^0 cells by growth on raffinose. This signaling-mediated mimic of carbon source substitution improves the chronological viability of ρ^+ and ρ^0 cells and may be analogous to lifespan extension of ρ^+ yeast by glycerol (Wei et al., 2009). Energy deprivation likely underlies accelerated chronological aging of ρ^0 cells. Trehalose, which accumulates in *reg1Δ mks1Δ* cells, but not *mks1Δ* or *reg1Δ* ρ^0 cells, could provide an energy store that ρ^0 cells use to increase lifespan. When energy generation is not compromised by respiratory deficiency, increased trehalose accumulation appears to be dispensable for increased viability (Figures 5C and 6A)

Beneficial effects of activation of the RTG response alone are evident both in lifespan extension of ρ^+ cells and increased oxidative stress resistance of SP ρ^0 cells. Functional equivalents of some key components of the yeast RTG response have yet to be identified in humans (Srinivasan et al., 2010). Nonetheless, our findings suggest general principles that will merit consideration in the effort to improve dietary manipulation for the benefit of human health. These efforts would build on the development of nutritional interventions such as ketogenic diets and fasting that provide therapeutic benefit in the treatment of various human disorders (Wallace et al., 2010). The evidence that the RTG response serves an anaplerotic function by increasing α-ketoglutarate and glutamate synthesis during log phase (Butow and Avadhani, 2004; Chen and Kaiser, 2002; Dilova et al., 2002) and intracellular BCAA levels in SP provides a starting point for design of therapeutic supplementation schemes that mimic the positive effects of the *mks1Δ* mutation. Our results also highlight the importance of detailed understanding of the interplay between signaling pathways that are modulated by a beneficial nutritional intervention. While coordinate activation of Snf1 signaling and the RTG response through deletion of *MKS1* and *REG1* improves the fitness of ρ^0 cells, deletion of *REG1* alone is detrimental to both ρ^+ and ρ^0 cells. Pharmacological strategies that attempt to imitate dietary interventions are likely to encounter similar hurdles.

EXPERIMENTAL PROCEDURES

Strains and Cell Culture

Chromosomal deletion mutants (Table S1) were generated by one-step gene disruption. ρ^0 strains were obtained by two rounds of ethidium bromide selection. Cell culture was performed in batch at 30°C using standard media except where noted, and cell densities were estimated by spectrophotometry. Individual colonies were used to seed starter cultures that were grown overnight at 30°C to SP and then used to seed experimental cultures to 0.25 optical density 600 (OD_{600}) or lower. In statistical analyses, t-score to p value transformations took into account equality of variances. All sample means were calculated from at least three independent measurements, and except where noted in the Supplemental Information, p values are for two-sided tests.

Immunoblot Analyses of Bulk and Posttranslationally Modified Histones

Total protein was concentrated by trichloroacetic acid precipitation (Friis et al., 2009). Bulk histone tail modification was analyzed by immunoblotting of similar cell equivalents of protein using modification-specific antibodies (Table S2). Total H3, total H4, or actin served as loading controls.

Metabolic Profiling by ^{1}H-NMR

Cells were pelleted from 2.5-day YPD cultures, rapidly washed once in water, and flash frozen in liquid nitrogen. After cell lysis in pH 7.5 phosphate buffer by bead beating at 4°C (BioSpec minibeadbeater), supernatants were clarified by centrifugation (50,000 × *g* for 1 hr at 4°C), filtered (Amicon Ultra 0.5 ml centrifugal filters, 3 kDa cutoff; Millipore), and loaded into glass melting-point capillaries (0.8–1.1 × 90 mm; Kimble Chase). Sample-loaded capillaries were placed in 5 mm nuclear magnetic resonance (NMR) tubes with ~500 μl of reference solution containing 0.49 mM deuterated 2,2-dimethyl-2-silapentane-5-sulfonic acid (DSS-d_6; Chenomx) in 99.9% D_2O. For standard-volume NMR to measure glucose abundance, samples were prepared and filtered as above and then lyophilized. Samples were resuspended in 600 μl D_2O with 0.49 mM DSS-d_6 and loaded into 5 mm NMR tubes. One-dimensional ^{1}H-NMR spectra were acquired at 303 K on a 500 MHz Varian INOVA spectrometer using the standard two-pulse sequence with water presaturation in VnmrJ v3.2 (1 s preacquisition delay; 4 s acquisition; sweep width 14.0 ppm; 128 transients). Spectra were analyzed using Chenomx NMR Suite v7.0.

Acetyl-CoA Analysis by LC-MS/MS

A Bruker maXis Impact quadropole time-of-flight (QTOF) tandem mass spectrometer (MS/MS) (Bruker) equipped with a 1100 series HPLC system (Agilent Technologies) was used to quantify acetyl-CoA in cell extracts. A TOSOH TSKgel Amide-80 column (1.0 mm ID × 25 cm, 5 μm particle size) was used for chromatographic separation and the acetyl-CoA ions were detected using multiple reaction monitoring with the transition of the m/z 810 precursor ion to the m/z 303.13 product ion. To overcome the matrix effect, a standard addition method was used for acetyl-CoA quantification in the metabolite samples. See Supplemental Information for details.

ATP Assay

Approximately 2.0 × 10^7 cells were disrupted in lysis reagent from the ATP Bioluminescence Assay Kit HS II (Roche #11 699 709 001) by vortexing with glass beads (BioSpec Products #11079105). One-twentieth of this lysate was assayed with the same kit in a Perkin Elmer Enspire 2300 Multilabel Plate Reader according to the manufacturer's instructions.

In Vitro KAT Assay

Approximately 2.7 × 10^8 ρ^0 cells were harvested from 4-day YPD cultures, flash frozen in liquid nitrogen, and stored at −70°C. Cell pellets were resuspended in 500 μl of ice-cold assay buffer (75 mM Tris [pH 8.2], 150 mM NaCl, 0.1 mM EDTA, 2 mM β-mercaptoethanol, 100 μM phenylmethanesulfonylfluoride, and one tablet [per 10 ml of assay buffer] complete Mini EDTA-free protease inhibitor cocktail [Roche #04 693 159 001]). In independent assays, this buffer was additionally supplemented with 10 μM TSA (Sigma T1952), 1 mM sodium orthovanadate (Sigma S-6508), or both 10 μM TSA and 1mM sodium orthovanadate. After addition of 500 μl of 0.5 mm glass beads (BioSpec #11079105), cells were broken during four 1 min rounds of vortexing alternated with 1 min in ice water. Lysates were collected in fresh microfuge tubes and centrifuged at 14,000 rpm for 20 min at 4°C. After removing the supernatant, the pellet was resuspended in 400 μl of assay buffer. The resuspended pellet was then subjected to four 10 s rounds of sonication at 10% output on constant duty cycle (Branson Sonifier 450) alternated with 1 min on ice. Purified DNA obtained after sonication migrated between 2,000 bp and 75 bp when analyzed by gel electrophoresis (R.F. and M.S., unpublished data). Protein concentrations of sonicated lysates were determined using the Bio-Rad Protein Assay (Bio-Rad 500-0006). For each sample, two 100 μl reactions containing 50 μg of protein were prepared, one without and the other with acetyl-CoA. Reactions were stopped and proteins precipitated by bringing the reactions to 25% trichloroacetic acid followed by incubation on ice for 15 min. Precipitates were pelleted by centrifugation at 13,000 rpm for 10 min at room

temperature and washed overnight in acetone. Precipitates were resuspended in sample buffer and analyzed by immunoblotting as described above.

Chronological Aging

Cells from overnight cultures were seeded at 2×10^6/ml into complete minimal medium containing 2% glucose and a 4-fold excess of histidine, methionine, leucine, and uracil (modified from Treco and Lundblad, 1993). A constant volume of culture was plated every day and viability was measured as colony-forming units (CFU). Experiments were performed in triplicate, and 100% viability is the peak of colony-forming ability of an individual strain (note that the day of peak viability differs between strains). The interpretations based on this analysis are not substantially affected by consideration of standard plots (Fabrizio and Longo, 2003; Wei et al., 2011) in which 100% viability of each strain is the colony-forming ability at 3 days growth (Figure S4B).

Recombination

White colonies of CCFy100-derived strains (Roy and Runge, 2000) were selected from 2-day YPD plates. Approximately 1,000 CFU from overnight cultures, seeded to the same initial OD_{600}, were plated on YPD, incubated for 4 days, and then stored at 4°C for 1 week. The frequency of red and sectored Ade^- colonies was determined.

Oxidative Stress

YPD cultures seeded to the same initial OD_{600} were grown into SP (3 days) and then exposed to 0–100 mM H_2O_2 for 1 hr. Cells were resuspended and diluted in YP and a constant number plated on YPD in 5-fold serial dilution.

SUPPLEMENTAL INFORMATION

Supplemental Information includes Supplemental Experimental Procedures, four figures, and two tables and can be found with this article online at http://dx.doi.org/10.1016/j.celrep.2014.03.029.

ACKNOWLEDGMENTS

Funding was provided by the Canadian Institutes for Health Research (to B.S. and M.S.), the Natural Sciences and Engineering Research Council of Canada (to L.L.), and the Faculty of Medicine and Dentistry, University of Alberta (to M.S.). We are grateful to M. Werner-Washburne, M. Stark, L. Pillus, K. Runge, and J. Broach for strains and Darren Hockman for technical assistance.

Received: March 28, 2013
Revised: December 13, 2013
Accepted: March 10, 2014
Published: April 10, 2014

REFERENCES

Allard, S., Utley, R.T., Savard, J., Clarke, A., Grant, P., Brandl, C.J., Pillus, L., Workman, J.L., and Côté, J. (1999). NuA4, an essential transcription adaptor/histone H4 acetyltransferase complex containing Esa1p and the ATM-related cofactor Tra1p. EMBO J. *18*, 5108–5119.

Alvers, A.L., Fishwick, L.K., Wood, M.S., Hu, D., Chung, H.S., Dunn, W.A., Jr., and Aris, J.P. (2009). Autophagy and amino acid homeostasis are required for chronological longevity in Saccharomyces cerevisiae. Aging Cell *8*, 353–369.

Boudreault, A.A., Cronier, D., Selleck, W., Lacoste, N., Utley, R.T., Allard, S., Savard, J., Lane, W.S., Tan, S., and Côté, J. (2003). Yeast enhancer of polycomb defines global Esa1-dependent acetylation of chromatin. Genes Dev. *17*, 1415–1428.

Bryk, M., Banerjee, M., Murphy, M., Knudsen, K.E., Garfinkel, D.J., and Curcio, M.J. (1997). Transcriptional silencing of Ty1 elements in the RDN1 locus of yeast. Genes Dev. *11*, 255–269.

Burtner, C.R., Murakami, C.J., Kennedy, B.K., and Kaeberlein, M. (2009). A molecular mechanism of chronological aging in yeast. Cell Cycle *8*, 1256–1270.

Butow, R.A., and Avadhani, N.G. (2004). Mitochondrial signaling: the retrograde response. Mol. Cell *14*, 1–15.

Carmen, A.A., Rundlett, S.E., and Grunstein, M. (1996). HDA1 and HDA3 are components of a yeast histone deacetylase (HDA) complex. J. Biol. Chem. *271*, 15837–15844.

Chen, E.J., and Kaiser, C.A. (2002). Amino acids regulate the intracellular trafficking of the general amino acid permease of Saccharomycescerevisiae. Proc. Natl. Acad. Sci. USA *99*, 14837–14842.

Coons, D.M., Boulton, R.B., and Bisson, L.F. (1995). Computer-assisted nonlinear regression analysis of the multicomponent glucose uptake kinetics of Saccharomyces cerevisiae. J. Bacteriol. *177*, 3251–3258.

D'Antona, G., Ragni, M., Cardile, A., Tedesco, L., Dossena, M., Bruttini, F., Caliaro, F., Corsetti, G., Bottinelli, R., Carruba, M.O., et al. (2010). Branched-chain amino acid supplementation promotes survival and supports cardiac and skeletal muscle mitochondrial biogenesis in middle-aged mice. Cell Metab. *12*, 362–372.

Dilova, I., Chen, C.Y., and Powers, T. (2002). Mks1 in concert with TOR signaling negatively regulates RTG target gene expression in S. cerevisiae. Curr. Biol. *12*, 389–395.

Enjalbert, B., Parrou, J.L., Vincent, O., and François, J. (2000). Mitochondrial respiratory mutants of Saccharomyces cerevisiae accumulate glycogen and readily mobilize it in a glucose-depleted medium. Microbiology *146*, 2685–2694.

Epstein, C.B., Waddle, J.A., Hale, W., 4th, Davé, V., Thornton, J., Macatee, T.L., Garner, H.R., and Butow, R.A. (2001). Genome-wide responses to mitochondrial dysfunction. Mol. Biol. Cell *12*, 297–308.

Fabrizio, P., and Longo, V.D. (2003). The chronological life span of Saccharomyces cerevisiae. Aging Cell *2*, 73–81.

Flores, C.L., Rodríguez, C., Petit, T., and Gancedo, C. (2000). Carbohydrate and energy-yielding metabolism in non-conventional yeasts. FEMS Microbiol. Rev. *24*, 507–529.

Fraenkel, D.G. (1982). Carbohydrate metabolism. In The Molecular Biology of the Yeast Saccahromyces: Metabolism and Gene Expression, J.N. Strathern, E.W. Jones, and J.R. Broach, eds. (Cold Spring Harbor: Cold Spring Harbor Laboratory), pp. 1–37.

Friis, R.M.N., and Schultz, M.C. (2009). Untargeted tail acetylation of histones in chromatin: lessons from yeast. Biochem. Cell Biol. *87*, 107–116.

Friis, R.M.N., Wu, B.P., Reinke, S.N., Hockman, D.J., Sykes, B.D., and Schultz, M.C. (2009). A glycolytic burst drives glucose induction of global histone acetylation by picNuA4 and SAGA. Nucleic Acids Res. *37*, 3969–3980.

Fuchs, S., Bundy, J.G., Davies, S.K., Viney, J.M., Swire, J.S., and Leroi, A.M. (2010). A metabolic signature of long life in Caenorhabditis elegans. BMC Biol. *8*, 14.

Gottlieb, S., and Esposito, R.E. (1989). A new role for a yeast transcriptional silencer gene, SIR2, in regulation of recombination in ribosomal DNA. Cell *56*, 771–776.

Greaves, L.C., Reeve, A.K., Taylor, R.W., and Turnbull, D.M. (2012). Mitochondrial DNA and disease. J. Pathol. *226*, 274–286.

Hallstrom, T.C., and Moye-Rowley, W.S. (2000). Multiple signals from dysfunctional mitochondria activate the pleiotropic drug resistance pathway in Saccharomyces cerevisiae. J. Biol. Chem. *275*, 37347–37356.

Hedbacker, K., and Carlson, M. (2006). Regulation of the nucleocytoplasmic distribution of Snf1-Gal83 protein kinase. Eukaryot. Cell *5*, 1950–1956.

Hedbacker, K., and Carlson, M. (2008). SNF1/AMPK pathways in yeast. Front. Biosci. *13*, 2408–2420.

Kyryakov, P., Beach, A., Richard, V.R., Burstein, M.T., Leonov, A., Levy, S., and Titorenko, V.I. (2012). Caloric restriction extends yeast chronological lifespan by altering a pattern of age-related changes in trehalose concentration. Front Physiol *3*, 256.

Lemercier, C., Legube, G., Caron, C., Louwagie, M., Garin, J., Trouche, D., and Khochbin, S. (2003). Tip60 acetyltransferase activity is controlled by phosphorylation. J. Biol. Chem. *278*, 4713–4718.

Liu, Z., and Butow, R.A. (1999). A transcriptional switch in the expression of yeast tricarboxylic acid cycle genes in response to a reduction or loss of respiratory function. Mol. Cell. Biol. *19*, 6720–6728.

Liu, Z., Sekito, T., Spírek, M., Thornton, J., and Butow, R.A. (2003). Retrograde signaling is regulated by the dynamic interaction between Rtg2p and Mks1p. Mol. Cell *12*, 401–411.

Martin, F.P., Spanier, B., Collino, S., Montoliu, I., Kolmeder, C., Giesbertz, P., Affolter, M., Kussmann, M., Daniel, H., Kochhar, S., and Rezzi, S. (2011). Metabotyping of Caenorhabditis elegans and their culture media revealed unique metabolic phenotypes associated to amino acid deficiency and insulin-like signaling. J. Proteome Res. *10*, 990–1003.

Mayer, F.V., Heath, R., Underwood, E., Sanders, M.J., Carmena, D., McCartney, R.R., Leiper, F.C., Xiao, B., Jing, C., Walker, P.A., et al. (2011). ADP regulates SNF1, the Saccharomyces cerevisiae homolog of AMP-activated protein kinase. Cell Metab. *14*, 707–714.

McBrian, M.A., Behbahan, I.S., Ferrari, R., Su, T., Huang, T.W., Li, K., Hong, C.S., Christofk, H.R., Vogelauer, M., Seligson, D.B., and Kurdistani, S.K. (2013). Histone acetylation regulates intracellular pH. Mol. Cell *49*, 310–321.

Minard, K.I., and McAlister-Henn, L. (2010). Pnc1p supports increases in cellular NAD(H) levels in response to internal or external oxidative stress. Biochemistry *49*, 6299–6301.

Morano, K.A., Grant, C.M., and Moye-Rowley, W.S. (2012). The response to heat shock and oxidative stress in *Saccharomyces cerevisiae*. Genetics *190*, 1157–1195.

Morrish, F., Noonan, J., Perez-Olsen, C., Gafken, P.R., Fitzgibbon, M., Kelleher, J., VanGilst, M., and Hockenbery, D. (2010). Myc-dependent mitochondrial generation of acetyl-CoA contributes to fatty acid biosynthesis and histone acetylation during cell cycle entry. J. Biol. Chem. *285*, 36267–36274.

Mullen, J.R., Kayne, P.S., Moerschell, R.P., Tsunasawa, S., Gribskov, M., Colavito-Shepanski, M., Grunstein, M., Sherman, F., and Sternglanz, R. (1989). Identification and characterization of genes and mutants for an N-terminal acetyltransferase from yeast. EMBO J. *8*, 2067–2075.

Nwaka, S., and Holzer, H. (1998). Molecular biology of trehalose and the trehalases in the yeast Saccharomyces cerevisiae. Prog. Nucleic Acid Res. Mol. Biol. *58*, 197–237.

Ocampo, A., Liu, J., Schroeder, E.A., Shadel, G.S., and Barrientos, A. (2012). Mitochondrial respiratory thresholds regulate yeast chronological life span and its extension by caloric restriction. Cell Metab. *16*, 55–67.

Petti, A.A., Crutchfield, C.A., Rabinowitz, J.D., and Botstein, D. (2011). Survival of starving yeast is correlated with oxidative stress response and nonrespiratory mitochondrial function. Proc. Natl. Acad. Sci. USA *108*, E1089–E1098.

Ron, D., and Walter, P. (2007). Signal integration in the endoplasmic reticulum unfolded protein response. Nat. Rev. Mol. Cell Biol. *8*, 519–529.

Roy, N., and Runge, K.W. (2000). Two paralogs involved in transcriptional silencing that antagonistically control yeast life span. Curr. Biol. *10*, 111–114.

Sadowski, I., Breitkreutz, B.J., Stark, C., Su, T.C., Dahabieh, M., Raithatha, S., Bernhard, W., Oughtred, R., Dolinski, K., Barreto, K., and Tyers, M. (2013). The PhosphoGRID Saccharomyces cerevisiae protein phosphorylation site database: version 2.0 update. Database (Oxford) *2013*, bat026.

Sandmeier, J.J., French, S., Osheim, Y., Cheung, W.L., Gallo, C.M., Beyer, A.L., and Smith, J.S. (2002). RPD3 is required for the inactivation of yeast ribosomal DNA genes in stationary phase. EMBO J. *21*, 4959–4968.

Schüller, H.J. (2003). Transcriptional control of nonfermentative metabolism in the yeast Saccharomyces cerevisiae. Curr. Genet. *43*, 139–160.

Seker, T., Møller, K., and Nielsen, J. (2005). Analysis of acyl CoA ester intermediates of the mevalonate pathway in Saccharomyces cerevisiae. Appl. Microbiol. Biotechnol. *67*, 119–124.

Sinclair, D.A., and Guarente, L. (1997). Extrachromosomal rDNA circles—a cause of aging in yeast. Cell *91*, 1033–1042.

Smets, B., Ghillebert, R., De Snijder, P., Binda, M., Swinnen, E., De Virgilio, C., and Winderickx, J. (2010). Life in the midst of scarcity: adaptations to nutrient availability in Saccharomyces cerevisiae. Curr. Genet. *56*, 1–32.

Smith, J.S., and Boeke, J.D. (1997). An unusual form of transcriptional silencing in yeast ribosomal DNA. Genes Dev. *11*, 241–254.

Srinivasan, V., Kriete, A., Sacan, A., and Jazwinski, S.M. (2010). Comparing the yeast retrograde response and NF-κB stress responses: implications for aging. Aging Cell *9*, 933–941.

Takahashi, H., McCaffery, J.M., Irizarry, R.A., and Boeke, J.D. (2006). Nucleocytosolic acetyl-coenzyme a synthetase is required for histone acetylation and global transcription. Mol. Cell *23*, 207–217.

Treco, D.A., and Lundblad, V. (1993). Basic techniques of yeast genetics. In Current Protocols in Molecular Biology, F.M. Ausubel, R. Brent, R.E. Kingston, D.D. Moore, J.G. Seidman, J.A. Smith, and K. Struhl, eds. (New York: John Wiley and Sons), pp. 13.11.11–13.11.17.

Wallace, D.C., Fan, W., and Procaccio, V. (2010). Mitochondrial energetics and therapeutics. Annu. Rev. Pathol. *5*, 297–348.

Wei, M., Fabrizio, P., Madia, F., Hu, J., Ge, H., Li, L.M., and Longo, V.D. (2009). Tor1/Sch9-regulated carbon source substitution is as effective as calorie restriction in life span extension. PLoS Genet. *5*, e1000467.

Wei, M., Madia, F., and Longo, V.D. (2011). Studying age-dependent genomic instability using the S. cerevisiae chronological lifespan model. J. Vis. Exp. *55*, 3030.

Wellen, K.E., Hatzivassiliou, G., Sachdeva, U.M., Bui, T.V., Cross, J.R., and Thompson, C.B. (2009). ATP-citrate lyase links cellular metabolism to histone acetylation. Science *324*, 1076–1080.

Wilson, W.A., Hawley, S.A., and Hardie, D.G. (1996). Glucose repression/derepression in budding yeast: SNF1 protein kinase is activated by phosphorylation under derepressing conditions, and this correlates with a high AMP:ATP ratio. Curr. Biol. *6*, 1426–1434.

Yuan, H., Rossetto, D., Mellert, H., Dang, W., Srinivasan, M., Johnson, J., Hodawadekar, S., Ding, E.C., Speicher, K., Abshiru, N., et al. (2012). MYST protein acetyltransferase activity requires active site lysine autoacetylation. EMBO J. *31*, 58–70.

Zaman, S., Lippman, S.I., Zhao, X., and Broach, J.R. (2008). How Saccharomyces responds to nutrients. Annu. Rev. Genet. *42*, 27–81.